Trails of OH emissions from small comets near Earth

L. A. Frank and J. B. Sigwarth

Department of Physics and Astronomy, The University of Iowa, Iowa City

Abstract. The results are reported for a successful search for the OH emissions associated with an influx of small comets into Earth's upper atmosphere with a camera on board the Polar spacecraft. The spatial distributions of the OH emissions are characterized by a bright core of intensities at or less than the spatial resolution of the camera which is surrounded by a larger dim region of luminosities. The Earth's shadow is employed in order to obtain a coarse determination of the altitudes of these OH trails, i.e., an altitude range < 3000 km.

Introduction

We use a camera on the Polar spacecraft to observe the emissions of the OH radical which is produced by the photodissociation of water by solar radiation in the water clouds from the disruption of small comets. Because there is no strong fluorescence emissions from water at ultraviolet and visible wavelengths the OH emissions act as proxy for the presence of the cometary water molecules. These OH emissions are a bright component of the host of emissions from well–known large comets [Feldman, 1996].

Instrumentation and observations

On 24 February 1996 the Polar spacecraft was launched into an eccentric orbit with perigee and apogee altitudes of 5170 km and 50,510 km, respectively, an orbital period of 17.6 hours, and an inclination of 86°. This spacecraft was equipped with a despun platform which allows the Visible Imaging System (VIS) to stare at Earth. The VIS is composed of three cameras, the Earth Camera for far–ultraviolet emissions, and two cameras for visible wavelengths, the Low–Resolution Visible Camera and the Medium–Resolution Visible Camera [*Frank et al.*, 1995]. These cameras for visible wavelengths are serviced with a filter wheel with twelve individual filters. Of present interest is the filter at 308.5 nm with passband width of 5.6 nm. This filter is sensitive to the solar resonance fluorescence from the OH radical in the (0, 0) band of $A^2\Sigma^+ - X^2\Pi$. Images from the Low–Resolution Visible Camera are presented here. The field–of–view of this camera is 5.4° × 6.3° and is serviced by an intensified charge–coupled device (CCD). The CCD provides an array of 256 × 256 picture elements (pixels), each with field–of–view of about 0.023° × 0.023°. The fields–of–view of the visible cameras could be placed at any position within a field–of–view of 20° × 20° via a mirror which is pointed with a bi–axial motor drive.

The inability to balance the spacecraft mass produced a cyclic motion of the angular pointing of the platform with amplitude of 0.38° and period of 6 s. The projection of this circular motion onto the image planes of the cameras produced two bright ansae for a point source. The ansae are always aligned along the X–axis of the images from all of the VIS cameras. For the Low–Resolution Visible Camera the corresponding amplitude of this undesired motion is 16.5 pixels, and insufficient for resolving the cometary water clouds. Hence the instrument's onboard computers were reprogrammed to sample only one of the two bright ansae and thus restore the angular resolution of the camera.

An example of the detection of the OH trail due to the motion of a cometary water cloud is given in Figure 1. This image was taken at 0410 UT on 31 December 1996. The spacecraft altitude was 30,300 km at geographic latitude and longitude of 51.4N and 226.3E, respectively. There are three detections shown in this frame for the following reason. The total sampling period is 13.5 s and is composed of three brief snapshots of 1 s each. For an object with constant apparent speed the three detections must be collinear, have equal separations and be of very similar magnitudes. This is a marvelously simple and constrained method of separating these sightings from the source of image contamination, i.e., the deposition of charge due to the penetration of energetic charged particles in the sensor. This method was also employed during subsequent observations of OH trails on 22 February and 13 March 1997 for which the OH filter was periodically replaced with other filters. The filters included those for the detection of the sodium D–lines and cometary dust. No sodium or dust trails were detected. The Earth is viewed only at nighttime because viewing the enormous intensities of the dayside would quickly destroy the sensor. The OH intensities in Earth's nighttime atmosphere are generally below the sensitivity of the camera. The superposed geographical image is generated by a commercial software package (see Acknowledgments). The apparent angular speed of the trail is 0.035°/s.

A pixel map for the three snapshots is shown in Figure 2. DN is the pixel contents in units of digitization numbers. Our method for snapshots does not uniquely determine which snapshot was the first one. Figure 2 does demonstrate the severe constraints on secure identification of a trail, i.e., the collinearity, the equal

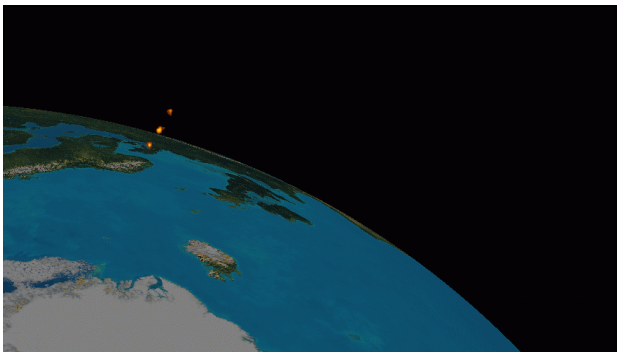

Figure 2. Three consecutive snapshots of the OH emissions at 308.5 nm which are associated with the motion of a cometary water cloud above Earth's atmosphere. The snapshots were taken at 0410 UT on 31 December 1996. The three snapshots have been superposed onto an image of Earth.

spacing, and the similar intensities. An additional criterion that can be applied, if necessary, is the fact that a false event due to charge deposition from a penetrating charged particle exhibits very discontinuous amplitude variations as a function of adjacent pixels.

The image of Figure 1 is suggestive that the OH trails are positioned at relatively low altitudes. In order to provide evidence that the trails are most frequently at the lower altitudes, two special series of images were obtained. The intent was to use Earth's shadow as the tool for determining the general altitude range of the trails because the emissions are being detected as solar fluorescence radiation. The first series of images placed the camera's field–of–view generally in a position for which the cometary water clouds were likely to be exposed to sunlight. During the period 0058–0223 UT on 22 February 1997, 37 images were taken with the 308.5–nm filter. The number of trail detections and their positions with respect to the CCD array are shown in Figure 3. During this time the spacecraft is moving with respect to Earth, but in order to avoid unnecessary complexity in this graphical summary, the Polar position for the center frame at 0139 UT is used at altitude 39,150 km and geographic latitude and longitude, 63.9N and 214.2E, respectively. The minimum altitudes are shown for the range of 0 to 3000 km, along with our planet's geometric shadow. The circles for these minimum altitudes are given for the viewing cones with apex at the spacecraft position. Thus the viewing geometry for the minimum altitudes and Earth's limbs is the same as for a viewer located at the position of the Polar spacecraft. The position of the terminator is also shown in Figure 3, along with the projection of the solar direction. Note that, for apparent positions in the shadow, the trail must be located at a minimum distance greater than that shown in the figure. Each dot in Figure 3 represents three snapshots of the same trail with position given for the center snapshot. There are 15 bright and 2 dim trails. Also note that, as the lower right–hand corner of the image frame is approached, and thus the shadow position, there is a relative paucity of trails. In order to further test this shadowing of the cometary water clouds from the solar radiation, a second series of images were obtained during 1953–2121 UT on 13 March 1997. The field–of–view was moved deeper into Earth's shadow. The results are shown in Figure 4. The spacecraft position for the center frame at 2038 UT was an altitude of 36,075 km and 57.8N and 268.0E. Even though the number of frames, 48, was greater than that for Figure 3, the number of bright and dim trails were only 3 each, significantly less than for the frames taken out of the shadow zone. A few sightings of the OH trails are expected because the shadow is a cylindrical volume extending in the antisolar direction and in this projection a few of the objects can be located outside of the shadow. This evidence places a large fraction of the trails at altitudes of 2000 to 3000 km or less.

Discussion

Our interpretation of these remarkable OH–radical trails at 308.5 nm is directed toward a specific example, that of 0410 UT on 31 December 1996 of Figure 2. The quantitative aspects of the interpretation are not different for the other trails. Inspection of the snapshot labeled 2 in Figure 2 finds that there appears to be two general features in the luminosities, an intense

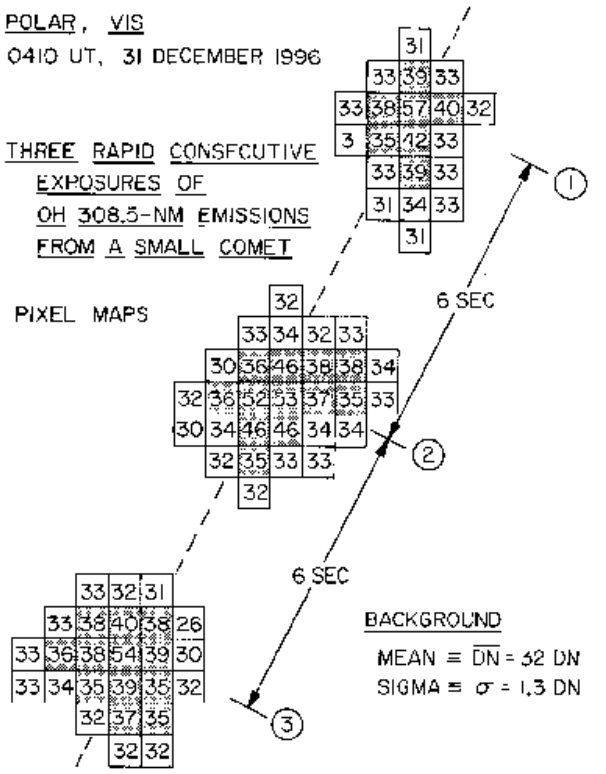

Figure 1. Pixel maps for the three snapshots of the OH trail shown in Figure 1.

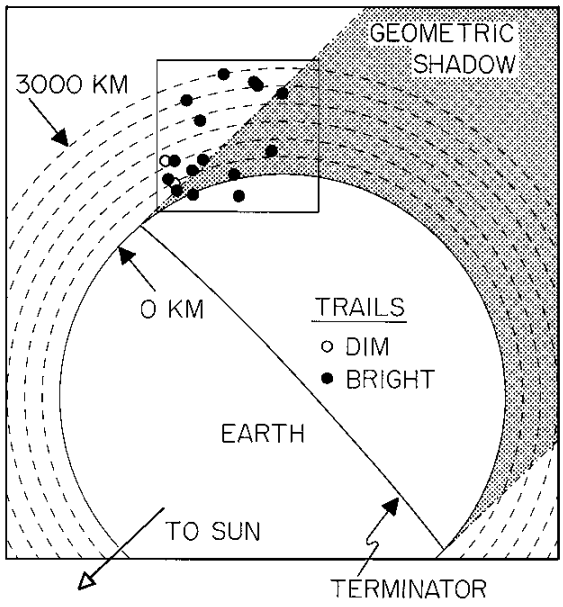

Figure 3. A summary of the OH trail detections for the period 0058 to 0223 UT on 22 February 1997. Each solid or open circle represents a set of three snapshots. The geometric shadow of Earth is shown in order to provide a coarse overview for the expectations of significant shadowing of the solar light if the cometary water clouds are at low altitudes.

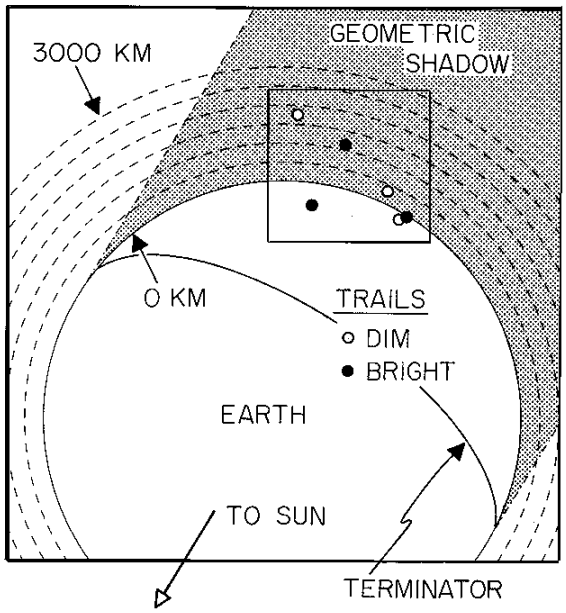

Figure 4. Continuation of the OH survey for the period 1953 to 2121 UT on 13 March 1997. The image frames are taken considerably deeper into Earth's shadow.

core and a diffuse background surrounding this core. It should be noted that the pixel background responses are quite flat with a mean of 32 DN and a σ of only 1.3. This σ includes all sources of noise with the exception of that due to the deposition of charge in the pixel sites by the passage of an energetic charged particle. The right–hand border of snapshot 3 has been compromised by such a charged particle event and the corresponding pixel values are not shown. Most of these latter events were removed with a software filter which detects brightened pixels or areas with intensity boundaries that are too sharp to be consistent with the image of a real object in the field–of–view.

The details of the acquisition of the three snapshots in Figure 2 are considered here. The motion of the object between two snapshots is 9.5 pixels during the spin period of 6 s. The accumulation time for an image spans a period of 1.362 s. In chronological order the image is accumulated for 0.388 s, then the electronic shutter is closed for 0.352 s, and the image is accumulated for an additional period of 0.622 s. Thus the snapshot is accumulated for 1.010 s. The center of the ansa is crossed at 0.681 s from the beginning of the accumulation interval. The camera is shuttered because otherwise the scattered sunlight from the booms would overwhelm the intensities from the OH–emitting object. The frame accumulation period is necessarily placed at an intensity ansa due to the unbalanced camera platform motion as the spacecraft rotates. The above sampling mode provides a "despinning" of the image from an uncompensated 16.5 pixels in the horizontal direction in Figure 2 to about 2.0 pixels. The accumulation period of 1.362 s corresponds to an object motion along the direction of motion in Figure 2 of about 2.2 pixels. These inaccuracies are about the same as the dimensions of the point spread function for a star as viewed with the same mode of operation. Thus the bright cores of the three snapshots shown in Figure 2 are consistent with a point source in terms of the camera's resolution.

The diffuse dim glow which extends out to pixels with responses ranging from 38 DN to 33 or 34 DN in Figure 2 is due to an extended source.

The apparent angular speed of the OH trail in Figure 1 is about 0.035°/s and is typical of most of such trails. At a range of 30,000 km the apparent speed is then about 18 km/s. The typical range of such trail speeds is about 5 to 15 km/s, and thus similar to the apparent speeds of atmospheric holes [*Frank and Sigwarth*, 1993, 1997a].

The interpretation of the bright core of intensities is discussed first. An intensity of 56 photons/cm^2–s at the entrance aperture of the camera corresponds to 1 DN in each of the three snapshots shown in Figure 2. For the bright core of snapshot 2 its five bright pixels correspond to a total of 83 DN after subtraction of the mean background signal of 32 DN each pixel. The bright core responses of other trails are typically within factors of 0.5 to 2 of this value. The 308.5–nm photon flux at the camera's entrance aperture is $f = 4.6 \times 10^3$ photons/cm^2–s. The photon emission at the source is then $S = 4\pi R^2 f$

where R is the distance to the source in cm, about 30,000 km or 3×10^9 cm. Then S = 5.2×10^{23} photons/s. If an intermediate value for the g–factor for the emission of 308.5–nm radiation in sunlight is taken as g = 5×10^{-4}/s [*Schleicher and A'Hearn*, 1982] then the total number of OH radicals in the source region is N_{OH} = S/g = $(5.2 \times 10^{23})/(5 \times 10^{-4}) = 1.0 \times 10^{27}$. The mass of this number of OH radicals is about 2.8×10^4 g. If this amount of OH is to be interpreted in terms of the disruption of a small comet and subsequent expansion and photodissociation of the water molecules due to solar radiation then the amount of water molecules required for a photodissociation lifetime τ_d of 8.2×10^4 s and a time interval after disruption of the comet of 50 s is $N_{H_2O} = N_{OH}$ $(8.2 \times 10^4)/(50) = 1.6 \times 10^{30}$ H_2O molecules, or 4.8×10^7 g. The time interval for the comet disruption is estimated from the fact that it must be at least 13 s from Figure 2 and less than 78 s because the same trail is not seen in the next consecutive image. If a simplified model of the H_2O as homogeneous in a disk with one pixel (12 km) in radius and oriented with face perpendicular to the camera's line–of–sight is assumed, then the column densities are about 3.5×10^{17} H_2O molecules/cm^2, or about 1.8 optical depths, which does not preclude this simple model.

The bright core of intensities is likely to be due in part to the prompt emission from OH radicals in highly excited rotational levels in the wavelength range 280 to 330 nm [*Budzien and Feldman*, 1991]. The relevant branching ratio is 0.011 and a fraction ~0.2 of these emissions are passed through the visible camera's filter. A simple model of the water cloud formation after the comet's disruption, i.e., a homogeneous disk with radial expansion speed v_e, finds that the water vapor at time t is $N_w = 1.8 \times 10^{18}$ $v_e^2 t^3$ [*Frank and Sigwarth*, 1997b] and the OH–radical rate is $N_w/\tau_d = 2.2 \times 10^{13}$ $v_e^2 t^3$ OH radicals/s. At time t the total number of OH radicals is N_{OH}) 5.5×10^{12} $v_e^2 t^4$. The source strength S_p for prompt emissions is (0.011×0.2) N_w/τ_d) 4.8×10^{10} $v_e^2 t^3$ photons/s. The source strength for fluorescence is $N_{OH} \times g = 2.8 \times 10^9$ $v_e^2 t^4$. The ratio of the emissions is S_p/S_f) 17/t. Thus for expansion speeds in the range of 0.5 km/s it is quite possible to account for the bright core by prompt emissions at early times, or correspondingly at distances of 10 to 20 km from the center of the vaporizing cloud. To sustain the brightness of the core shown in Figure 1 and 2 with prompt emissions, the OH production rate is 2.4×10^{26}/s. At times in the range of 30 to 100 s (at the larger distances from the core and in the diffuse region) the emissions will be dominated by resonance fluorescence.

There is a third possible interpretation of the bright core of intensities in the OH pixel maps in Figure 2. Trails of atomic oxygen emissions at 130.4 nm were detected with the Earth Camera on board the Polar spacecraft [*Frank and Sigwarth*, 1997b]. These trails were interpreted in terms of the direct release of atomic oxygen during disruption of the small comet because the short trail lifetimes and the water and oxygen optical depths were inconsistent with the standard dissociation model as discussed above. A discussion of the various laboratory and other evidences for the production and storage of atomic oxygen in icy bodies in the solar system is given by *Frank and Sigwarth* [1997b]. The complete light curve for the OH emissions from the small comets is not determined with the current images. However, the possibility that the OH radicals are directly stored in the cometary body and produced over time by similar sputtering cannot be excluded. There is laboratory evidence that OH can be stored in water ices [*Cooper and Abbatt*, 1996]. In order to account for the OH emissions for snapshot 2 in Figure 1, the required mass is about 3×10^4 g. In this case the mass of the small comet is not determined because the ratio of water and OH radicals is not known. Ratios of 10^2 and 10^3 are probably not unreasonable and imply small comet masses in the range of 3×10^6 to 3×10^7 g. It is noted that the OH is highly reactive and is expected to rapidly combine with other cometary constituents such as carbon. The above estimate for the OH content will be higher if the OH lifetime is short after release by disruption.

The dim, extended region of OH emissions shown in Figure 2 is of considerable interest. It is assumed to also cover the bright cores. The area of the dim glow has a diameter of 4 to 5 pixels. The sum of the pixel responses in this area is about 50 DN. Thus the flux at the camera is f = 2.8×10^3 photons/cm^2–s and the source S = 3.2×10^{23} photons/s. The corresponding number of OH radicals is about 6.4×10^{26} and, with the standard model for photodissociation by solar radiation, the water vapor content is 1.0×10^{30} H_2O molecules for a time of 50 s after disruption. The corresponding mass of water snow prior to disruption is about 3.0×10^7 g. The pixel dimensions are 12 km × 12 km. Thus the diameter of the diffuse emissions is then about 50 to 60 km, and similar to that for atmospheric holes as viewed in the dayglow with the Earth Camera. With the simplifying assumption of a homogeneous distribution of the water molecules in a disk with diameter 50 km and aligned with its plane perpendicular to the line–of–sight of the Polar cameras the column densities are 5.1×10^{16} H_2O molecules/cm^2 within an estimated accuracy of a factor of 2.

The above mass of the distribution of water molecules in the dim, diffuse region of OH emissions, 3.0×10^7 g, is similar to the mass estimates for small comets as given recently by *Frank and Sigwarth* [1993]. The above simple model of the water density in the diffuse disk with diameter of about 50 km gives a column density of 5.1×10^{16} H_2O molecules/cm^2. The optical depth is about 0.25. These estimates are given for a time 50 s after the small comet's disruption. As noted above, the possible range of times is 13 to 78 s. The corresponding range of cometary water mass is 1.2×10^8

g and 1.9×10^7 g, respectively, both for a disk diameter of 50 km. The corresponding optical depths are about 1.0 and 0.16, respectively. The typical optical depth for the water cloud which is responsible for atmospheric holes is in the range of about 0.5. Thus the amount of water vapor which is calculated by using the OH emissions as a proxy is sufficient to account for the atmospheric holes.

Summary

The Low–Resolution Visible Camera on board the Polar spacecraft was successfully employed to detect the trails of OH radicals at 308.5 nm which are due to the presence of cometary water clouds at altitudes in the range of 3000 km or less above Earth's surface. The OH emissions which are a well–established proxy for the presence of water vapor exhibit two spatial features, a relatively bright central core and a dimmer region surrounding the core. The diameter of the dim, diffuse region is about 50 km which is similar to the diameters of the transient decreases of far–ultraviolet dayglow, or atmospheric holes, as observed by the Earth Camera. There was no evidence for the presence of sodium or dust as would be expected for the well–known larger comets such as Comet Hale–Bopp which was also viewed by the Polar camera. It is important to note that the observed occurrence frequency of the OH trails is similar to that for atmospheric holes as would be expected if the holes are due to absorption of the far–ultraviolet dayglow by cometary water clouds. Global rates of both of these phenomena are in the range of 5 to 30 events/minute.

Acknowledgments. The snapshots of the cometary water clouds were superposed onto FACE OF THE EARTH™ (copyright © 1996, ARC Science Simulations). This research was supported in part at The University of Iowa by NASA Contract NAS5–30316.

References

Budzien, S. A. and P. D. Feldman, "OH prompt emission in Comet IRAS–Araki–Alcock (1983VII)", *Icarus, 90,* 308–318, 1991.

Cooper, P. L. and J. P. D. Abbatt, "Heterogenous interactions of OH and HO_2 radicals with surfaces characteristic of atmospheric particulate matter", *J. Phys. Chem., 100,* 2249–2254, 1996.

Feldman, P. D., "Comets", in *Atomic, Molecular, & Optical Physics Handbook,* ed. G. W. F. Drake, pp. 930–939, American Institute of Physics, Woodbury, NY, 1996.

Frank, L. A. and J. B. Sigwarth, "Atmospheric holes and small comets", *Rev. Geophys., 31,* 1–28, 1993.

Frank, L. A., et al., "The visible imaging system (VIS) for the Polar spacecraft", *Space Sci. Rev., 71,* 297–328, 1995.

Frank, L. A. and J. B. Sigwarth, "Transient decreases of Earth's far–ultraviolet dayglow", *Geophys. Res. Lett.*, (this issue), 1997a.

Frank, L. A. and J. B. Sigwarth, "Detection of atomic oxygen trails of small comets in the vicinity of Earth", *Geophys. Res. Lett.*, (this issue), 1997b.

Schleicher, D. G. and M. F. A'Hearn, "OH fluorescence in comets: Fluorescence efficiency of the ultraviolet bands", *Ap. J., 258,* 864–877, 1982.

L. A. Frank and J. B. Sigwarth, Department of Physics and Astronomy, The University of Iowa, Van Allen Hall, Iowa City, IA 52242.
(e-mail: frank@iowasp.physics.uiowa. edu; sigwarth@iowasp.physics.uiowa.edu)

(Received April 8, 1997; revised July 25, 1997; accepted July 29, 1997.)